Isotopic ordering in adsorbed hydrogen monolayers

M. Bienfait

CRMC2, Faculté des Sciences de Luminy, Case 901, F-13288 Marseille Cedex 9, France

P. Zeppenfeld

Johannes Kepler Universität Linz, Institut für Experimentalphysik, A-4049 Linz, Austria

R. C. Ramos, Jr.

Department of Physics, University of Washington, Seattle, Washington 98195

J. M. Gay

CRMC2, Faculté des Sciences de Luminy, Case 901, F-13288 Marseille Cedex 9, France

O. E. Vilches

Department of Physics, University of Washington, Seattle, Washington 98195

G. Coddens

Laboratoire Léon Brillouin, Centre d'Etude Saclay, F-91191 Gif-sur-Yvette, France

Quantum ordering, mixing, and mobility of isotopic hydrogen mixtures adsorbed on graphite (0001) is studied in the monolayer range by diffraction, small angle (SANS), and quasielastic neutron scattering (QENS). Solid mixtures of H_2-D_2 commensurate with the graphite substrate remain random isotopic mixtures from 18 K down to 3 K. Incommensurate solid mixtures of H_2-D_2 at monolayer completion with and without a partial second layer adsorbed on top show a tendency towards phase separation and clustering as the temperature is reduced below 20 K. This tendency is monitored both by the change of the diffraction peak intensity with temperature and by features of the SANS measurements discussed in the text. Clustering slows down or stops at $\simeq 8$ K without reaching the full isotopic phase separation predicted on quantum-mechanical grounds. The QENS measurements measured the mobility of pure HD and HD-D_2 mixtures for two coverages. The mobility in the mixture is enhanced over the one of pure HD at the same coverage and temperature, an effect which can be related to a bond softening of the heavier D_2 molecule due to quantum motion. [S0163-1829(99)01936-0]

I. INTRODUCTION

The mass difference between the molecular isotopes hydrogen (H_2), deuterium hydride (HD), and deuterium (D_2) leads to very different liquid-vapor (L-V) critical and liquid-vapor-solid (L-V-S) triple points in both three[1] and two dimensions.[2,3] This effect is due to the importance of the zero-point kinetic energy in these quantum systems and makes the hydrogen isotopic molecules have the lowest S-L-V triple points in nature. The zero-point kinetic energy also manifests itself in the freezing of binary isotopic mixtures by the observation of bulk quantum fractionation, i.e., the separation at freezing of a liquid enriched with the lower-mass isotopic molecule, and a solid rich in the larger mass isotope.[4]

The same quantum mass effect should also induce an isotopic ordering at low temperature in the bulk solid phase. Isotopic phase separation[5–7] was predicted a long time ago. It was observed for ^{3}He-^{4}He mixtures[8] but never for isotopic hydrogen solid solutions,[9] although it has been predicted to occur at temperatures as high as $\simeq 4$ K.[6,7]

Isotopic phase separation should be expected also in an adsorbed single layer of an isotopic hydrogen mixture. The reduced dimensionality and coordination number in a monolayer with respect to its three-dimensional counterpart makes the relative contribution of the zero-point kinetic energy to the total energy larger than in bulk. This is responsible, among other things, for a substantial difference in the molar areas of H_2 and D_2 at solidification and at monolayer completion.[2,3] The difference in molar areas lifts the chemical equivalence of the isotopes and may lead to phase separation, estimated to occur at about 2 K.[10] Other forms of ordering have been predicted by theory for monolayer commensurate mixtures formed on graphite.[11]

Kinetic effects (low translational mobility in the solid phase), which may be responsible for the nonobservation of phase separation at low temperature in the bulk solid phase, may be overcome by the existence of non-negligible surface hydrogen mobility on thick films down to 3 K as observed by Mangele, Albrecht, and Leiderer.[12] and between 2 and 4 K as measured by Sukhatme, Rutledge, and Taborek.[13] Other observations[14,15] and calculations[16,17] show that a fraction of hydrogen adsorbed on top of a complete solid monolayer is mobile and favors the interlayer exchange and equilibrium between the first and second layers.

Progress in the last 5 years on the understanding of mono-

layers of the hydrogen molecular isotopes has been significant. Wiechert and co-workers[2,3] have compiled an extensive review of the currently accepted phases and phase diagrams within the first monolayer for the three species H_2, HD, and D_2 adsorbed on graphite. In the first monolayer, all three molecules form commensurate (CS) and incommensurate (IS) solid structures, as well as fluid phases at low densities and high temperatures. The formation of a CS phase preempts condensation into L-V coexistence, a L-V critical point, and a L-V-S triple point, in favor of a CS-V coexistence region that may extend down to $T=0$ K.

Double layers of hydrogen isotopic mixtures adsorbed on graphite were also studied by heat-capacity measurements.[14] It was shown that the first layer close to the substrate is strongly enriched in the heavier isotope.

The experiments reported in this paper were carried out by neutron scattering because it can distinguish between all three isotopic binary molecules H_2, HD, and D_2 and to characterize disordered mixtures, separated phases, and superlattice structures. The experiments take advantage of the large difference in the coherent and incoherent cross sections of the various hydrogen isotopes. Indeed, the contribution to the diffraction signal from all three isotopic molecules is significant since the coherent scattering length of both H (-3.742 fm) and D ($+6.674$ fm) are large, yet it is of opposite sign. On the other hand, the large incoherent scattering length of H (especially in the HD molecule, which does not undergo ortho-para conversion at low temperatures) can be used to measure the liquid fraction in a liquid-solid coexistence regime[18] and to determine the diffusion coefficient in the liquid.

The work reported here was intended to study binary mixtures of the hydrogen isotopic molecules adsorbed on graphite searching for the possible fractionation at solidification and for the expected isotopic phase separation in the solid phase at low temperature. We performed three kinds of neutron-scattering experiments at various CS and IS surface densities (ρ), molar concentrations (x), and temperatures (T).

(i) Diffraction experiments were performed on H_2-D_2 mixtures to identify long-range ordering in the solid phase and its possible evolution with temperature.

(ii) Small-angle neutron-scattering (SANS) investigations were carried out on monolayer H_2-D_2 mixtures. SANS is sensitive to the temperature dependence of the short- and medium-range structural and compositional order within the mixture.[19–21] We were thus looking for the formation of small clusters of D_2 and H_2.

(iii) Quasielastic neutron-scattering (QENS) experiments were performed on HD-D_2 mixtures to measure the incoherent scattering function of the HD molecules at high temperature (15, . . . ,30 K). These measurements yield the self-correlation function of the HD molecules in the fluid phase and hence the corresponding diffusion coefficient.[15,18,22]

The diffraction measurements mapped portions of the ρ, T, $x=n(H_2)/[n(H_2)+n(D_2)]$ parameter space and were complemented by the SANS and QENS experiments. Clustering, a first step towards phase separation, was investigated further with the SANS measurements. With the QENS we looked for— but did not find—any indication of fractionation during the L-S transition. Instead, a rather unexpected

effect was observed: by substituting one half of HD by the heavier molecule D_2 in an adsorbed monolayer, we measured an enhancement of the hydrogen mobility with respect to the pure HD layer in the fluid phase just above the melting temperature.

After describing the experimental details, we report on the diffraction and SANS experiments, then on the QENS measurements, and finally, we conclude with a discussion on the interpretation of our results. Preliminary reports on some of our findings have been published recently.[10,23]

II. EXPERIMENT

The small-angle neutron-scattering and the neutron-diffraction experiments were performed on the G6.1 diffractometer at the Laboratoire Léon Brillouin (LLB) (Saclay) using a wavelength $\lambda = 4.74$ Å and a scattering vector range 0.13 Å$^{-1}<Q<2.54$ Å^{-1}. They were complemented by SANS measurements and diffraction experiments carried out on the D16 ($\lambda=4.51$ Å; 0.13 Å$^{-1}<Q<0.6$ Å^{-1}) and D1B ($\lambda=2.52$ Å; 1.7 Å$^{-1}<Q<4.3$ Å^{-1}) spectrometers at the Institute Lave Langevin (ILL) (Grenoble). All experiments gave consistent and reproducible results within the experimental uncertainty.

The gases used where H_2 (purity 99.999%) and D_2 (purity 99.8%). Mixtures with various x were prepared in a calibrated volume, and the gas was slowly introduced in the sample cell held at 25 K. The cell was then cooled down to 20 K. After allowing the H_2 ortho-para conversion to reduce the incoherent background, the temperature was decreased step by step down to the lowest value that could be reached with the cryostat (2.8 K at the LLB and 1.5 K at the ILL). In this temperature range, the neutron scattering from para H_2 is essentially coherent. As for the other isotope, D_2 is known to be a good coherent scatterer at all temperatures.

The QENS experiments were performed on the time-of-flight spectrometer MIBEMOL at the LLB (Saclay). The incident wavelength was 8 Å (1.28 meV) with a triangular-shaped resolution function of 40 μeV full width at half maximum (FWHM). The scattered beam was measured by 10 detector banks located at scattering vectors Q ranging from 0.35 to 1.46 Å^{-1}.

The gas mixture used for the QENS measurements was composed of HD and D_2. Deuterium hydride HD (purity 97.7%) has a temperature-independent large incoherent scattering cross section ($\sigma_{HD}^{inc}=60$ b) well suited for measuring the self-correlation scattering function and studying the surface mobility of the HD molecules in adsorbed layers.[14,18,22] Deuterium has a much smaller incoherent scattering cross section ($\sigma_{D}^{inc}=2.0$ b), which can be neglected in the QENS analysis. The HD-D_2 mixtures were adsorbed as described above, annealed at 30 K for 2 h and cooled down to the temperature of the neutron-scattering recording (15 K$<T$ <30 K).

For all diffraction and QENS experiments, the final scattering spectra were obtained after subtracting the background due to the cell and the bare graphite substrate. We noticed that the background signal is essentially temperature independent.

For the substrate, we used a recompressed exfoliated graphite known as Papyex.[24] Two samples were used; they

consisted of stacks of disks, 22 mm in diameter and several cm high, having masses of 33.5 g and 28.5 g, respectively, placed in cylindrical thin-wall aluminum cells. The macroscopic Papyex surfaces were parallel to the scattering plane.

The total surface area of the two samples was determined by measuring a CH_4 adsorption isotherm at 77.3 K prior to the neutron-scattering experiment.[10,23] We assumed that the inflexion point located at the middle of the plateau connecting the first and second steps (reflecting the condensation of the first and second layer) would correspond to the completion of the $(\sqrt{3} \times \sqrt{3})R30°$ commensurate CH_4 monolayer ($\rho = 1$). As a matter of fact, this assumption led to an underestimation of the coverage by about 20% (Refs. 25 and 26) as we realized by measuring N_2 adsorption isotherms at 77.3 K. All the coverages quoted in Refs. 10 and 23 have been recalibrated here. Hence, the former $\rho = 1.6$ corresponds to $\rho = 1.92$, the former $\rho = 1$ to $\rho = 1.2$, and the former $\rho = 0.9$ to $\rho = 1.08$. This coverage recalibration does not change the qualitative conclusions about the trend towards phase separation at large coverages drawn from our preliminary reports.[10,23] The absolute dosing is known within a few percent.

On dealing with the different isotopic molecules and their mixtures, the first layer completion densities are different for each one of them. We give dosings in units of the commensurate coverage since it corresponds to a given number of molecules per unit area, independent of the type of hydrogen isotopic molecule and for any sample cell. In these units, monolayer completion (incommensurate solid) for the three isotopic molecules are: $\rho = 1.46$ for H_2, $\rho \approx 1.49$ for HD, and $\rho = 1.55$ for D_2.

III. RESULTS

A. Neutron-diffraction and SANS measurements

1. Diffraction measurements

Monolayer mixtures at coverages $\rho = 1$, 1.08, 1.2, 1.54, and 1.92 have been studied as a function of temperature and H_2 molar fraction x. In the commensurate regime, we selected $x = 1/2$ for $\rho = 1$ and $x = 1/3$ (i.e., a composition $1/3 H_2 : 2/3 D_2$) for $\rho = 1.08$.

In the incommensurate regime, diffraction measurements have been performed for $x = 0.5$ for several coverages near $\rho = 1.2$ and at the pure D_2 monolayer completion ($\rho = 1.54$). For $\rho = 1.92$, i.e., for the fully compressed incommensurate structure with an excess of about $\rho = 0.4$ in the second layer, neutron-diffraction spectra have been recorded for $x = 0.2$, 0.33, 0.5, 0.8, and 0.9. We also measured the diffraction lines of pure D_2 and pure H_2 at $\rho = 1.92$ as a reference for the peak intensity and position measurements.

At $\rho = 1$ and 1.08, we observed the expected commensurate (10) lines at 1.70 $Å^{-1}$ for 2 K$<T<$18 K. Higher-order (11) and (20) peaks were also observed, but no superstructure lines were detected. The intensities of the (10) lines correspond to the calculated intensities of a commensurate compositionally disordered mixed crystal (see below). The $(\sqrt{3} \times \sqrt{3})R30°$ CS remains a H_2-D_2 random mixture down to ~ 2 K.

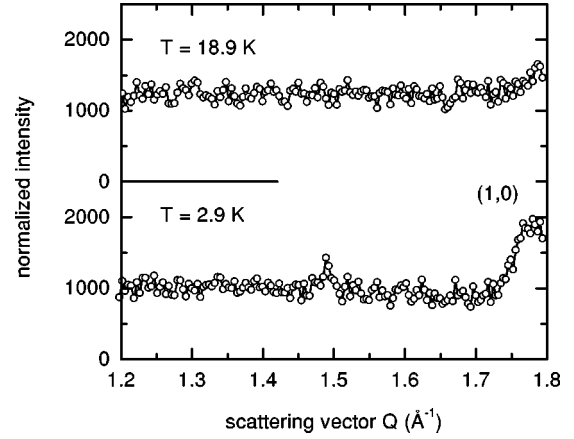At $\rho = 1.2$, the layer is slightly compressed with respect to the commensurate structure; we found a (10) line at

FIG. 1. Diffraction spectra for a 0.5 H_2:0.5 D_2 mixture for $\rho = 1.2$ adsorbed on graphite (0001) at 18.9 K and 2.9 K (graphite background subtracted). In the upper curve (18.9 K) a small bump at $Q = 1.77$ $Å^{-1}$ corresponding to a fluid phase is visible, whereas two peaks at 1.48 $Å^{-1}$ and 1.77 $Å^{-1}$ are observed in the lower curve ($T = 2.9$ K).

1.77 $Å^{-1}$, and in addition, we could discern at low temperature a small superstructure peak at 1.48 $Å^{-1}$ (see Fig. 1). Such a feature could be due to a structure similar to the γ solid observed by Wiechert and co-workers[2] for D_2 at this coverage and at low temperature. In this phase, the adlayer exhibits a periodic, static strain modulation. This kind of structural ordering observed at low temperature may be responsible for the concomitant decrease of the SANS signal (see Sec. III A 2).

For $\rho = 1.54$ and $\rho = 1.92$, the diffraction results look qualitatively the same; since we performed many more experiments at $\rho = 1.92$, we will focus our report on the patterns recorded for this coverage. A typical example is presented in Fig. 2 for $\rho = 1.92$, $x = 0.5$, and five different temperatures (20, 16, 12, 8, and 3 K). Another set of runs can be found in Ref. 10. A single (10) line is observed, which is located in the range between $Q = 2.07$ $Å^{-1}$ and $Q = 2.12$ $Å^{-1}$, corresponding to the position of the diffraction lines for pure H_2 and D_2, respectively.[2] No additional diffraction peaks were observed, except the higher-order (11)
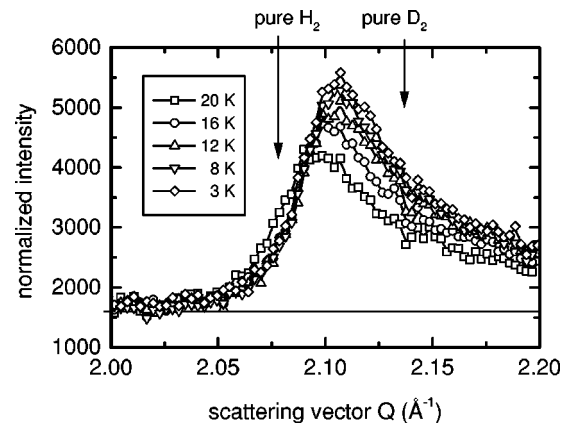

FIG. 2. (10) diffraction lines for a 0.5 H_2:0.5 D_2 mixture at $\rho = 1.92$ adsorbed on graphite (0001) for five different temperatures (graphite background subtracted). The solid lines are guides to the eye.
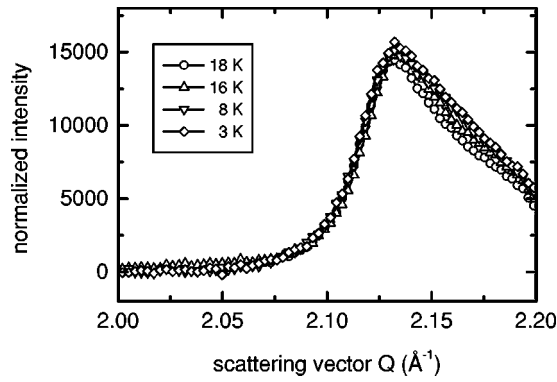
FIG. 3. Same as Fig. 2, but for a pure D_2 film with $\rho = 1.92$. Note that although the excess D_2 in the second layer solidifies at about 11 K there is no substantial contribution to the scattered intensity.

FIG. 4. Peak maxima of the (10) diffraction lines for different coverages at low temperature as a function of the molar fraction of H_2. The intensities are normalized to the intensity of a pure D_2 phase with the same total coverage. Circles, commensurate solid; squares, incommensurate solid at $\rho = 1.92$. The solid and dotted lines are the calculated intensities for a perfectly (random) mixed crystal [Eq. (1)] and for a fully phase-separated system [Eq. (2)], respectively.

and (20) lines. The (1,0) peak shifts towards the position characteristic of pure H_2 with increasing hydrogen content x. A slight shift of about 0.01 Å^{-1} towards larger Q for a given x is observed upon decreasing the temperature from 20 to 12 K. The (10) peak FWHM is almost independent of both x and T, and its value of about 0.06 Å^{-1} is similar to the one measured previously on H_2 or D_2 diffraction patterns on Papyex.[2,10] Hence, in the studied temperature range, the isotopic mixing does not strongly affect the overall long-range order in this two-dimensional (2D) crystal, at least within the instrumental resolution. This suggests that the disorder is mainly substitutional (stoichiometric) rather than positional (crystallographic).

The most striking change with decreasing temperature is the large increase of the intensity of the diffraction peak. As shown below (and supported by the SANS results presented in the next section), this intensity decrease can be attributed to H_2, D_2 cluster formation within the 2D mixture. In fact, the clustering could also explain the small shift of the diffraction line towards the position of pure D_2—the component with the larger scattering cross section.[27]

If the layer was *completely* phase separated, the expected ratio between the intensity of the H_2-pure and D_2-pure diffraction peaks would be roughly $(b_H/b_D)^2 \simeq 1/3$, and we should observe the two peaks at the locations indicated by the arrows in Fig. 2. Unfortunately, the experimental linewidth (0.06 Å^{-1}) is close to the peak separation. On the other hand, an *incompletely* phase-separated system is expected to be composed of domains (clusters or islands) of the pure constituents, which would not extend over a size even close to the transfer width, thus giving rise to a peak located at an intermediate position corresponding to the "average" lattice.[27] Hence, the absence of a peak splitting is *not* a proof against clustering, i.e., a trend towards phase separation at low temperatures.

The analysis of the temperature dependence of the diffraction intensities can help to clarify this point. The variation of the peak intensity with temperature for the mixture is much larger than for pure D_2 and H_2 as is evident by comparing Fig. 2 for the mixture and Fig. 3 for pure D_2. For the pure D_2 the change in intensity between 18 and 8 K is only 5%, and then it remains almost constant at lower temperature. Thi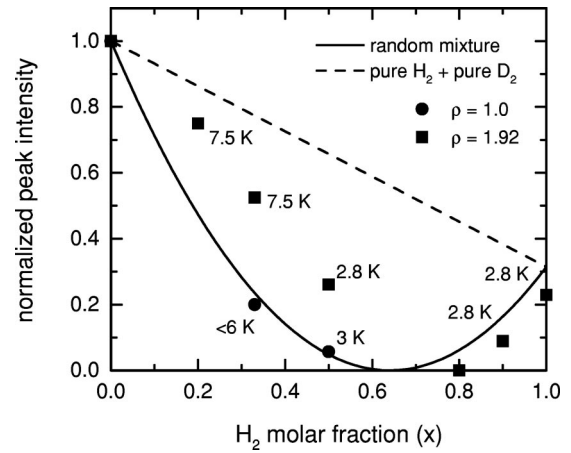s small variation can be accounted for by the Debye-Waller factor. Conversely, for the mixture (Fig. 2), the variation of the peak intensity with temperature is much stronger. The intensity increases by 40% between 20 and 8 K and by another 6% between 8 and 3 K. This point will be examined further below.

The peak intensity varies strongly with the molar fraction x, as well. This variation is expected from the different relative contributions b_H and b_D to the structure factor. Figure 4 presents the relative intensity of the peak maximum at low temperature as a function of x for different total coverages normalized to the expected intensity for pure D_2. Two lines are also shown. The solid line is the calculated intensity for a compositionally disordered adlayer (random mixture), according to

$$\frac{I}{I_{D_2}} = \frac{[xb_H + (1-x)b_D]^2}{b_D^2}, \tag{1}$$

whereas the dotted line describes the intensity for a fully phase-separated system, as given by

$$\frac{I}{I_{D_2}} = \frac{xb_H^2 + (1-x)b_D^2}{b_D^2}. \tag{2}$$

The calculated intensity for the random mixture reaches zero for $x = 0.64$ as a result of the opposite signs of b_H and b_D, respectively.

The measured intensities (peak maxima) at low temperature in the commensurate regime ($\rho = 1.08$, $x = 1/3$, and $\rho = 1$, $x = 1/2$) as well as at monolayer completion ($\rho = 1.92$, $x = 0.8$, and 0.9) are in fair agreement with the mixed-crystal model. However, the measured intensities for $\rho = 1.92$ and $x = 0.2$, 1/3, and 0.5 are much larger than those predicted by Eq. (1). In fact, they are intermediate between the values calculated for the randomly mixed and the fully phase-separated system. This observation, together with the strong increase of the intensity for $x = 0.2$, 1/3, and 0.5 with
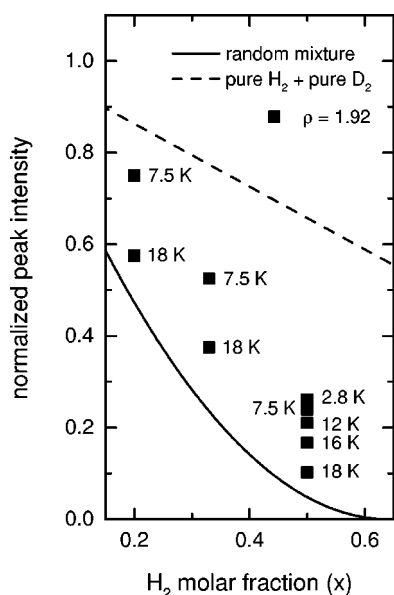
FIG. 5. Same as Fig. 4, but including the temperature variation of the diffraction peak intensities for $\rho = 1.92$.

decreasing temperature (see Figs. 2 and 5), suggests that strong H_2-H_2 and D_2-D_2 correlations are present in the 2D mixed phase. In other words, the H_2-D_2 two-dimensional mixture shows a trend towards phase separation at low temperature for these physical conditions ($\rho = 1.92$; $x = 0.2$, 1/3, and 0.5).

We have used a well-known formalism[28] to analyze the sawtoothlike shape of our diffraction spectra. A typical fit is shown in Fig. 6. The fits allow us to determine the coherence length L of the 2D crystal ($L \simeq 300$ Å) and the ''true'' peak position Q_0 of the diffraction lines (which is always located at slightly lower Q than the position of the peak maximum due to the asymmetry of the sawtooth profile). The values obtained for $x = 0$ (pure D_2) and 1 (pure H_2) agree perfectly
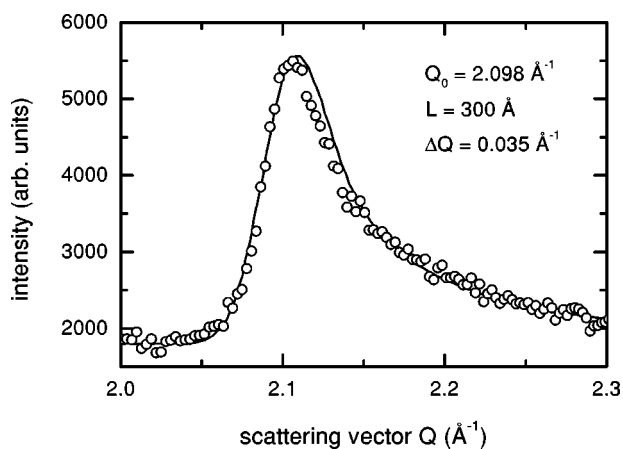

FIG. 6. Fit of the sawtoothlike diffraction peak recorded at 3 K for $\rho = 1.92$ and a molar fraction $x = 0.5$ using the model of Stephens *et al.* (Ref. 28). The results of the fit yield the exact position $Q_0 = 2.098$ Å^{-1} and the coherence length $L \simeq 300$ Å. The experimental resolution is $\Delta Q = 0.035$ Å^{-1} as measured from the width of the (0002) graphite substrate diffraction peak. The calculation takes into account the preferential orientation of the graphite surfaces in the Papyex sample.
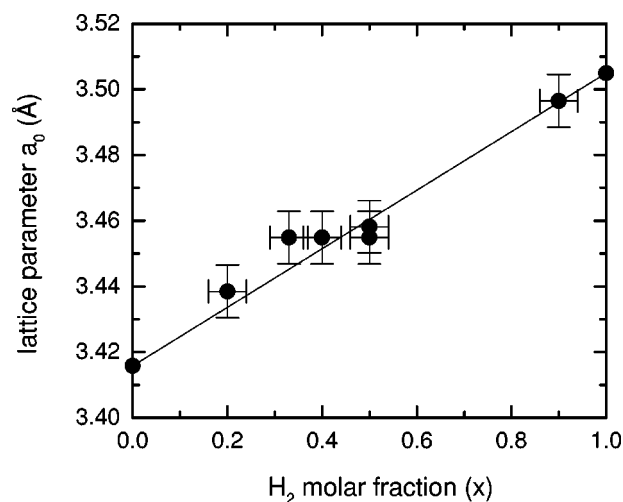

FIG. 7. Lattice parameter a_0 calculated from the position Q_0 of the (10) diffraction line as a function of the H_2 molar fraction at $\simeq 3$ K for $\rho = 1.92$. The straight line corresponds to Vegard's law, an expected linear relationship for mixtures of components with very similar lattice parameters in the pure state.

with those quoted in Refs. 2 and 3 for monolayer completion, being 2.124 and 2.070 Å^{-1}, respectively. The lattice parameter is calculated from the peak position Q_0 of the (10) diffraction line through $a_0 = 4\pi/(\sqrt{3}Q_0)$. The results for the pure and mixed phases are presented in Fig. 7 as a function of x. The values show, within experimental error, a linear dependence on x (Vegard's law).

2. SANS results

As described in the Introduction, the SANS technique can be used, for instance, to determine the size of small clusters or inclusions in a matrix[19–21] and its evolution upon heat treatment. In our case, we have measured the variation of the SANS intensity from 20 to about 3 K by decreasing the temperature step by step. After each step, we had to wait several hours before the scattering signal remained constant. We selected five coverages: $\rho = 1.92$, 1.54, 1.2, 1.08, and 1 for a molar concentration $x = 0.5$ (i.e., a composition 0.5 H_2:0.5 D_2). At 20 K, the adlayer is condensed either in a dense fluid ($\rho = 1, 1.08, 1.2$) or in a solid phase ($\rho = 1.54, 1.92$). We noticed a nonnegligible attenuation of the graphite background signal at small angle upon adsorption of the hydrogen mixture. In order to eliminate the contribution of beam absorption without tedious self-shielding corrections, we chose to represent the difference between SANS spectra recorded at different temperatures, as, for instance, $I(3$ K$)$-$I(20$ K$)$, shown in Fig. 8.

Figure 8 reveals that the influence of temperature on the SANS intensities depends strongly on coverage. For large coverage, i.e., at monolayer completion ($\rho = 1.54$) or above ($\rho = 1.92$), the SANS signal is larger at low temperature than at 20 K. At $\rho = 1.2$, the temperature variation is just reversed. We find a *decrease* of the SANS signal at low temperature.

The increase of the SANS signal at low temperature for $\rho = 1.92$ and 1.54 can be interpreted as being due to an isotopic clustering in the mixture. This trend towards phase separation was observed from $T = 8$ K downwards; the increase of the small-angle scattering intensity almost reaches
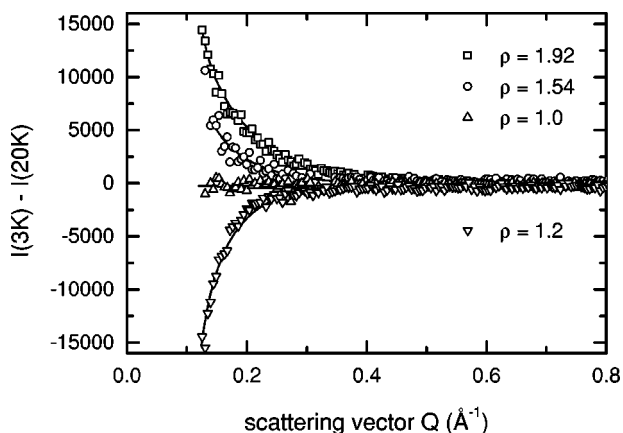
FIG. 8. Difference of small-angle neutron-scattering (SANS) spectra obtained from hydrogen isotopic H_2-D_2 mixtures (molar fraction $x=0.5$) adsorbed on graphite at $\simeq 3$ K and 20 K for different coverages $\rho=1.92$, 1.54, 1.0, and 1.2. The increase of the SANS intensity for low temperature is indicative of clustering within the 2D solid solution whereas the decrease observed at $\rho=1.2$ suggests that the layer becomes more ordered upon decreasing the temperature from 20 to 3 K.

its maximum at 8 K; any further temperature decrease to 3 K only increases the signal by a few percent, even after waiting for two days. This indicates that the process of phase separation, initiated by the formation of small H_2 and D_2 clusters, slows down at low temperature.

The interpretation of the *decrease* of the SANS intensity observed for $\rho=1.2$ at low temperature is not as straightforward. It suggests that ordering is improved in the adsorbed layer at lower temperature. This reorganization does not seem to be related, e.g., to the fluid domain-wall transition occurring between 20 and 16 K (Ref. 2) because the SANS intensity did not change significantly in this temperature range. We also emphasize that desorption between 3 and 20 K is negligible because both the equilibrium pressure and the dead volume of the sample cell are small. A possible explanation of the behavior could be the formation of an ordered superstructure similar to the γ phase observed for pure D_2 in the same temperature and coverage range. This explanation is supported by the appearance of an additional diffraction peak at 1.48 Å^{-1} (see Fig. 1).

In the vicinity of the commensurate solid ($\rho=1$ and 1.08), the SANS intensity is essentially constant between 20 and 3 K. No change in the ordering is detected between these temperatures although there is a fluid-solid transition below 20 K. This means that the adsorbed layer remains compositionally disordered even if it solidifies in a $(\sqrt{3}\times\sqrt{3})R30°$ structure.

3. Discussion

A trend towards phase separation was clearly observed at large coverage and low temperature for several physical conditions ($\rho=1.54$, $x=0.5$ and $\rho=1.92$, $x=0.2$, 1/3, and 0.5) as predicted by Prigogine a long time ago for bulk H_2-D_2 mixtures.[5] This effect is even more pronounced for $\rho=1.92$ than for $\rho=1.54$ (see Fig. 8), indicating that the nonnegligible fraction promoted to the second layer plays an important role in facilitating clustering by the process of in-

terlayer exchange. The existence of about 20% of adsorbed molecules in the second layer (monolayer completion for pure H_2 and pure D_2 occurs at $\rho=1.46$ and $\rho=1.55$, respectively) raises the question of its influence on the scattering patterns. It has been inferred from heat-capacity data[14] that in a double layer of pure H_2 deposited on a preplated monolayer of D_2, the ''vertical'' phase separation persists in the region of two solid layers, with a small amount of H_2 mixing into the first layer, and a small amount of D_2 going to the second layer at finite temperature; there is no quantitative thermodynamic data for this interlayer mixing for the range of H_2 and D_2 fractions explored in this study. We expect that the fraction of the second layer is mainly composed of H_2, which remains in a liquid state down to $\simeq 6$ K. Hence, its contribution to the diffraction intensity down to 8 K (Fig. 2) is negligible. On the other hand, the major part of the intensity variation occurs between 20 and 8 K, which shows that this variation results essentially from a reorganization in the first solid layer.

It must also be pointed out that the promotion of primarily H_2 into the second layer leads to an overestimation of the molar fraction in the first layer by $x\simeq 0.05$ to 0.1, depending on the H_2 concentration. This would shift the experimental data points in Figs. 4 and 5 accordingly to the left, hence improving the agreement between Eq. (1)—the random mixture curve—and the experimental results at high temperature (Fig. 5). We may wonder whether this concentration shift could affect our interpretation. If we consider the diffracted intensity reported in Fig. 4 for $\rho=1.92$ at 2.8 K and $x=0.5$ and the largest possible concentration shift to $x=0.4$ due to the promotion of H_2 in the second layer, then the measured intensity would still be twice as large as the intensity expected for the random mixture (as observed, for instance, for the commensurate structure at $\rho=1.0$). This is a clear indication for positive H_2-H_2 and D_2-D_2 correlations in the solid monolayer at 2.8 and also at 7.5 K (Fig. 5). At 7.5 K we cannot invoke a contribution of the second layer to the diffraction peak because the H_2 second layer is liquid at this temperature.

More information can be obtained on the clustering process at monolayer completion by applying standard models used previously to describe the formation of aggregates from solid solutions.[19–21] We selected two models describing two-dimensional islands (flat disks) in different arrangements. One represents an isotropic distribution of 2D islands. In the second model, all islands are parallel to the scattering plane. The actual distribution due to the orientation of the graphite flakes is intermediate between these two extreme situations. A fit of the data in Fig. 8 at $\rho=1.92$ yields a radius of 20 ± 4 Å as the average from both models. The combined diffraction and SANS results seem to indicate that the IS monolayer is a heterogeneous phase containing small clusters enriched in H_2 or D_2. This may be interpreted as a tendency for phase separation. It is not clear whether the phase separation is incomplete because of a persisting residual miscibility or for kinetic reasons. We could again wonder whether the vertical phase separation of the two isotopes could account for the observed SANS signal. At 8 K the SANS spectra for $\rho=1.92$ and 1.54 are similar to the one recorded at 3 K. However, since the H_2-rich fraction in the second layer is liquid

at 8 K, it cannot exhibit a ∼20 Å medium-range order. This is another reason why we can exclude the observed clustering to occur within the second layer only.

The clustering effect was not observed for several physical conditions recalled below.

(i) $\rho = 1.92$ and $x = 0.8$ and 0.9. This can be related to the smaller quantum volume of the D_2 molecule with respect to H_2; a small D_2 concentration (large x) can be easily dissolved in a H_2 matrix.

(ii) In the commensurate solid for $x = 1/3$ and 0.5. A calculation performed by De Mello and Massunaga[31] shows that the trend towards phase separation depends on the layer density and is indeed less favorable for the commensurate mixture.

(iii) At $\rho = 1.2$ and $x = 0.5$, we observe an *increase* of the ordering within the mixture (Fig. 8). This effect was not anticipated at all and could possibly be due to a superstructure formation.

B. QENS measurements

Our principal aims in the QENS experiments were to observe a possible ordering or phase separation at freezing of an isotopic hydrogen mixture adsorbed on graphite and to model the experimental spectra to determine the nature of the diffusive motion of HD in pure HD and of HD in the HD-D_2 mixture. As recalled in the Introduction, the HD molecule is well suited to measure the incoherent scattering function $S_{inc}(\mathbf{Q}, \omega)$ from which the translational diffusion coefficient and the mean residence time between jumps on the surface[15,18,22,29] can be determined. The incoherent scattering function is given by

$$S_{inc}(\mathbf{Q}, \omega) = j_0^2(Qr) \frac{1}{\pi} \frac{f(\mathbf{Q})}{f^2(\mathbf{Q}) + \omega^2} \exp(-Q^2 \langle u^2 \rangle), \quad (3)$$

where j_0, the spherical Bessel function of zeroth order, describes the isotropic rotational motion of the HD molecule with a gyration radius $r = 0.37$ Å. $\mathbf{Q}$ is the scattering vector, and $\hbar\omega = E - E_0 = \Delta E$ is the gain or loss of energy of the neutron with respect to the incident energy E_0. The exponential term is the Debye-Waller factor; the mean-square displacement $\langle u^2 \rangle$ for HD under our experimental conditions is about 0.20 Å.[22] The width $f(\mathbf{Q})$ of the Lorentzian depends on the model of molecular diffusion, as described below.

If some fraction of the HD film remains solid, the broad component of $S_{inc}(\mathbf{Q}, \omega)$ must be weighted by the liquid fraction, and an incoherent elastic contribution proportional to the solid part of the HD adlayer has to be added to Eq. (3). The theoretical scattering function must be integrated over the orientation distribution of the graphite crystallites and folded with the triangular-shaped QENS instrumental resolution function, before being fitted to the measured spectra.

Two QENS runs were carried out at the LLB-Saclay on MIBEMOL. Due to the limited allocated beam time and the long sampling times (10–20 h) required to accumulate data with reasonable statistics, we limited our measurements to two coverages in the incommensurate coverage regime, $\rho = 1.44$ and $\rho = 1.2$, and several temperatures above and below the ''melting'' temperature. We first checked with a pure HD layer that a measurable broadening of the scattered spec-
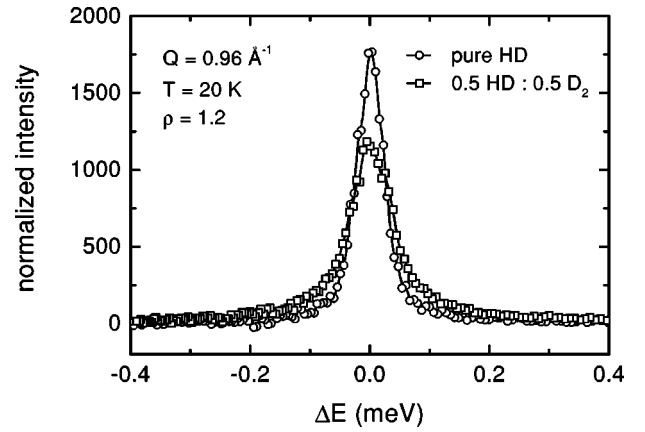

FIG. 9. Quasielastic neutron-scattering (QENS) spectra from a 0.5 HD:0.5 D_2 mixture and a pure HD adlayer for the same total coverage $\rho = 1.2$, $T = 20$ K, and $Q = 0.96$ Å^{-1}. The intensity of the spectrum recorded for the mixture is multiplied by a factor 2; in both cases the graphite background was subtracted.

tra could be obtained. For $\rho = 1.44$, the recorded broadening at $T = 29.1$ K, just above the melting temperature [26.5 K for HD, 25 K for D_2 (Refs. 2 and 3)], is small but slightly larger than the instrumental resolution. Thus we focused our measurements at $\rho = 1.2$ on a temperature range above and below the domain-wall fluid $\leftrightarrow$ fluid transition [$T = 19 \pm 1$ K for HD and D_2 (Refs. 2 and 3)] where, indeed, measurable wings could be observed for the HD fluid phase. The major part of the QENS experiments were performed at this coverage, at temperatures between 15 and 30 K and for the pure and mixed ($x = 0.5$) layers. The spectra obtained in both experimental runs were reproducible.

For $\rho = 1.2$, the spectra reveal a continuous variation of the broadening with temperature for both pure and mixed layers showing that some mobility still exists in the domain-wall fluid phase. Below the transition temperature ($\simeq 19$ K), the corresponding mobility resembles that of a viscous fluid. The limited resolution of the MIBEMOL instrument did not allow us to observe any clear indication of a solid-fluid coexistence in this regime for the HD-D_2 mixture.

Still, the QENS broadening obtained for the pure HD and for the mixed HD-D_2 layers are significantly different, especially close to 19 K. Figure 9 displays two such QENS spectra recorded at 20 K. The scattering function obtained with the mixture ($x = 0.5$) is multiplied by a factor of 2 for comparison with the pure HD spectrum (the contribution of D_2 is negligible). It is evident that the mobility in the mixed film is larger, even though one half of the *lighter* molecules (HD) have been replaced by heavier molecules (D_2). This amazing result was not anticipated at all; it is analyzed quantitatively below.

A detailed picture of the diffusive motion of the HD molecules can be obtained by applying standard models used previously to describe the molecular diffusion in physisorbed films.[15,18,22,29] At small scattering vector ($Q < 1$ Å^{-1}), all models asymptotically yield the following expression for $f(\mathbf{Q})$ in Eq. (3):

$$f(\mathbf{Q}) = D Q_\parallel^2, \quad (4)$$

where D is the translational diffusion coefficient of the molecules, and $Q_\parallel$ is the component of **Q** parallel to the graphite surface. Equation (4) characterizes a 2D Brownian motion.

To exploit the data in the entire Q range and gain information about the diffusion mechanism, we can use more complicated expressions for $f(\mathbf{Q})$ introducing the discrete nature of lattice diffusion. For instance, if molecules jump from site to site on a regular hexagonal lattice,

$$f(\mathbf{Q}) = \frac{3 - \{\cos(\mathbf{Q} \cdot \mathbf{a}) + \cos(\mathbf{Q} \cdot \mathbf{b}) + \cos[\mathbf{Q} \cdot (\mathbf{a} + \mathbf{b})]\}}{3\tau},$$

(5)

where **a** and **b** are the lattice vectors, and τ is the mean residence time on a lattice site. The hexagonal lattice was chosen here because the liquidlike layer is expected to have a pseudohexagonal packing and because the underlying graphite substrate exhibits hexagonal symmetry, too. The diffusion coefficient D is related to τ by the Einstein relation (2D),

$$D = \frac{a^2}{4\tau},$$

(6)

where $a = |\mathbf{a}| = |\mathbf{b}|$ is the jump distance of a molecule between sites.

The resulting scattering function $S_{inc}(\mathbf{Q}, \omega)$ has only one adjustable parameter D at small Q [Brownian motion, Eq. (4)] or two adjustable parameters τ and a if the entire Q-range is explored and if a hexagonal lattice jump model is assumed. These two parameters can be reduced to one using Eq. (6) if D is first determined from the spectra at small Q according to Eq. (4). We recall that the scattering function must be averaged over all orientations of Q and convoluted with the triangular-shaped resolution function before comparison with the measured spectra.

1. Two-dimensional Brownian motion

The whole set of collected data have been tested against Eqs. (4) and (5). An example is presented in Fig. 10 for the HD-D_2 mixture at 20 K. The resulting values for the diffusion coefficients obtained for $Q \lesssim 1$ Å^{-1} are listed in Table I for the pure HD and the mixed layers at $\rho = 1.2$ for each temperature. They are also plotted in Fig. 11. One can see that the diffusion coefficient D for the mixture is always larger than for the pure HD fluid (or domain-wall fluid). The difference is most significant at low temperature ($T \lesssim 20$ K). From the Arrhenius plot, we can estimate the activation energy for diffusion of an HD molecule to be 12.5 ± 1.6 meV in pure HD and 7.5 ± 0.8 meV in the mixture. These observations are discussed in Sec. IV below.

We also reported in Table I two diffusion coefficients obtained for $\rho = 1.44$ and $\rho = 1.08$ of pure HD, at two different temperatures. Comparing these values with those collected at $\rho = 1.2$, it follows that the diffusion coefficients decrease with increasing coverage at constant temperature. This is clearly related to the density dependence of the free space available for the molecules to move.

2. Hexagonal lattice jump model

Equations (3) and (5) were used to characterize the local motion of HD molecules within the adsorbed layer for cov-
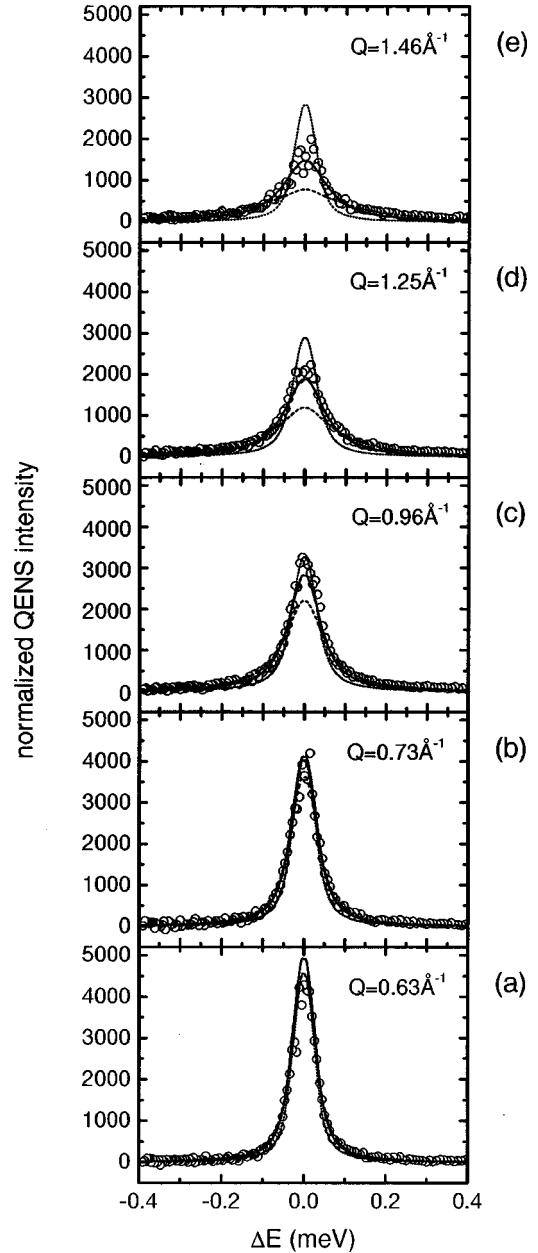

FIG. 10. QENS spectra of HD in a 0.5 HD:0.5 D_2 mixed layer adsorbed on graphite (background subtracted) at 20 K and a coverage $\rho = 1.2$ for different scattering vectors Q. The lines are fits to three models: two-dimensional Brownian motion (dotted line), hexagonal jump model with a lattice parameter $a = 3.9$ Å (dashed line), and $a = 2.46$ Å (solid line). The values of the parameters for the three models are $D = 1.1 \times 10^{-5}$ cm^2/s, $a = 3.9$ Å and $\tau = 3.5 \times 10^{-11}$ s, $a = 2.46$ Å and $\tau = 1.4 \times 10^{-11}$ s.

erage $\rho = 1.2$. We first selected a jump distance $a = 3.9$ Å, corresponding to the average distance between molecules at this coverage. From Eq. (6) and from Table I, we obtain the residence time τ for each physical condition. The obtained fit is good at small Q, as expected, but becomes poorer and poorer for $Q > 1$ Å^{-1}. This is illustrated in Fig. 10 for the mixed layer at 20.0 K. The calculated scattering function is too narrow, which means that the chosen jump distance a is too long.

Then, we selected a value $a = 2.46$ Å, corresponding to the distance between two nearest-neighbor hexagonal sites

TABLE I. Results for the best fits to the QENS spectra using the model of random translational diffusion (two-dimensional Brownian motion) described by Eq. (4). The diffusion coefficients D apply to the HD molecules in a pure HD or mixed 0.5 HD:0.5 D_2 layer for various coverages and temperatures.

pure HD $\rho = 1.2$		0.5 HD:0.5 D_2 $\rho = 1.2$	
T (K)	D (10^5 cm^{-2})	T (K)	D (10^5 cm^{-2})
15	<0.1	17.0	0.35
17.9	0.1	17.9	0.3
20.0	0.4	18.8	0.8
21.9	0.7	19.9	0.8
23.4	1.5	20.0	1.1
25.1	1.2	23.4	2.0
28.3	2.5	25.3	2.0
		29.5	3.0

$\rho = 1.08$	
T (K)	D (10^5 cm^{-2})
23.4	3.5

$\rho = 1.44$	
T (K)	D (10^5 cm^{-2})
29.1	0.2

TABLE II. Results for the best fits to the QENS spectra for pure HD and a 0.5 HD:0.5 HD mixture over the entire Q range using a hexagonal lattice jump model [Eq. (6)] for $\rho = 1.2$. The HD molecules are assumed to jump between nearest-neighbor hexagonal lattice sites ($a = 2.46$ Å) on graphite.

pure HD		0.5 HD:0.5 D_2	
T (K)	τ (10^{-11} s)	T (K)	τ (10^{-11} s)
17.9	8	17	2.5
21.9	2.2	20.0	1.4
28.3	0.6		

IV. DISCUSSION AND CONCLUSION

By using neutron-scattering techniques, we have obtained a microscopic view of the order (and disorder) in isotope hydrogen mixed single layers adsorbed on graphite. We also obtained some insight in the first stages of phase separation (clustering at low temperature).

At low temperatures, the evolution of the ordering strongly depends on coverage.

(i) For $\rho = 1.54$ and $\rho = 1.92$, i.e., at monolayer completion and above, a clustering is observed at 8 K and below. The neutron spectra show that the further evolution towards phase separation into the different isotopes is frozen out at 3 K. The complete phase separation could probably be achieved if the molecular motion could be activated. It is also important to emphasize that the presence of a large fraction (mainly H_2 in the second adsorbed layer) favors the formation of larger aggregates by the process of interlayer exchange.

(ii) For $\rho = 1.2$, the layer is more ''ordered'' at low temperature, but the data do not permit to decide whether the ordering is crystallographic and/or compositional.

(iii) In the vicinity of the commensurate coverage ($\rho \simeq 1$), the two-dimensional mixed lattice fluid transforms into a substitutionally disordered ($\sqrt{3} \times \sqrt{3}$)$R30°$ crystal with decreasing temperature.

At higher temperature (15–30 K), we have discovered an interesting behavior of the fluid monolayers close to the order-disorder transition by measuring the mobility of the HD molecules in a pure HD film and in a mixed HD-D_2 layer.

(i) For a pure ($\rho = 1.2$) monolayer of HD, we observed a continuous transition between the fluid and domain-wall fluid, in agreement with previous studies[2,3] and found the liquid-like mobility to persist in the domain-wall fluid. This result seems to be at variance with other studies,[30] which claimed, from diffraction and phonon measurements, that the domain-wall fluid phase is nothing else but a regular two-dimensional solid. As a matter of fact, our findings are not inconsistent with these previous results since the broad diffraction peaks that were observed there may also be interpreted as stemming from a highly correlated fluid.

(ii) For a 0.5 HD:0.5 D_2 mixture of the same coverage $\rho = 1.2$, we also observed a continuous transition and did not find any record of quantum fractionation. Still, the diffusion coefficient of the HD molecules in the mixed layer was found to be *larger* than in the pure film for the same coverage. This surprising result is probably related to the different

on the graphite surface, and proceeded as above to determine τ. The resulting curves nicely fit all sets of spectra (including large Q) for all temperatures both for the pure and mixed layers. Table II lists a few values of the so-determined residence times. We may conclude that the HD molecules perform jumps between nearest-neighbor hexagonal lattice sites on the graphite surface; their mean residence time in the graphite potential wells is in the 10^{-11} s range for temperatures around 20 K.
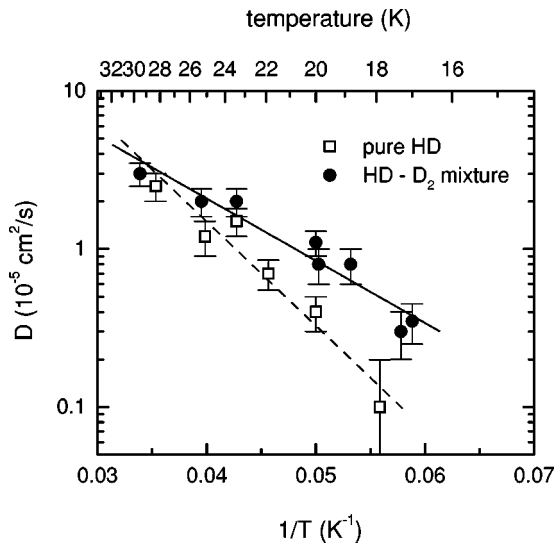

FIG. 11. Diffusion coefficient D of HD molecules versus inverse temperature $1/T$ in a pure HD (squares) and a mixed 0.5 HD:0.5 D_2 layer (circles) adsorbed on graphite (total coverage $\rho = 1.2$). The solid and dashed lines are the best fits to the data (circles and squares, respectively). The HD molecules are always more mobile in the mixture than in the pure HD adlayer.

temperatures of the order-disorder transitions for the pure HD and D_2 layer, respectively. The transition temperature is always smaller for the heavier molecule D_2 than for the lighter HD for coverages ranging from $\rho = 0.8$ to $\rho = 1.4$. This unexpected effect can be interpreted in terms of a strengthening of the bonding of the lighter molecule, resulting from its larger quantum motion.[31] Indeed, the lighter molecule has a larger vibrational amplitude, and it tends to experience more strongly the repulsive part of the van der Waals potential; this effect stabilizes the lighter isotope adlayer.

(iii) Finally, for both pure and mixed adlayers with $\rho = 1.2$, we found that the HD molecules jump between nearest-neighbor lattice sites on graphite. Hence, in these two-dimensional fluids, the short-range order is imposed by the underlying graphite lattice.

[1] See, e.g., the review by G. Baym and C. Pethick, in *The Physics of Liquid and Solid Helium*, edited by K. H. Benneman and J.B. Ketterson (Wiley, New York, 1978), Vol. 2.

[2] H. Freimuth, H. Wiechert, H. P. Schildberg, and H. J. Lauter, Phys. Rev. B **42**, 587 (1990); H. Wiechert, H. Freimuth, and H. J. Lauter, Surf. Sci. **269/270**, 452 (1992).

[3] H. Wiechert, in *Excitations in Two-Dimensional and Three-Dimensional Quantum Fluids*, edited by A. G. F. Wyatt and H. J. Lauter (Plenum, New York, 1991), p. 499; H. Wiechert, Physica B **169**, 144 (1991).

[4] See P. C. Souers, *Hydrogen Properties for Fusion Energy* (University of California, Berkeley, 1986).

[5] I. Prigogine, R. Bingen, and J. Jeener, Physica **20**, 383 (1954); 20**, 516 (1954); **20**, 633 (1954); I. Prigogine, *The Molecular Theory of Solutions* (North-Holland, Amsterdam, 1957), Chap. 19.

[6] W. J. Mullin, Phys. Rev. Lett. **20**, 254 (1968); **20**, 1550 (1968).

[7] W. J. Mullin and H. K. Sarin, Phys. Lett. **29A**, 49 (1969).

[8] D. O. Edwards, A. S. McWilliams, and J. G. Daunt, Phys. Rev. Lett. **9**, 195 (1962).

[9] S. N. Ischmaev, I. P. Sadikov, A. A. Chernyshov, G. V. Kobelev, V. A. Sukhoparov, and A. S. Telepnev, Zh. Éksp. Teor. Fiz. **102**, 711 (1992) [Sov. Phys. JETP **75**, 382 (1992)].

[10] M. Bienfait, P. Zeppenfeld, L. J. Bovie, O. E. Vilches, and H. J. Lauter, Physica B **234-236**, 159 (1997).

[11] G. M. Carneiro and E. V. L. de Mello, Phys. Rev. B **35**, 358 (1987).

[12] F. Mangele, U. Albrecht, and P. Leiderer, J. Low Temp. Phys. **96**, 177 (1996).

[13] K. Sukhatme, J. E. Rutledge, and P. Taborek, Bull. Am. Phys. Soc. **40**, 83 (1995).

[14] F. C. Liu, Y. M. Liu, and O. E. Vilches, Phys. Rev. B **51**, 2848 (1995).

[15] Y. M. Liu, P. S. Ebey, O. E. Vilches, J. G. Dash, M. Bienfait, J. M. Gay, and G. Coddens, Phys. Rev. B **54**, 6307 (1996).

[16] M. Wagner and D. M. Ceperley, J. Low Temp. Phys. **94**, 161 (1994).

[17] M. Wagner and D. M. Ceperley, J. Low Temp. Phys. **102**, 275 (1996).

[18] P. Zeppenfeld, M. Bienfait, F. C. Liu, O. E. Vilches, and G. Coddens, J. Phys. (France) **51**, 1929 (1990).

[19] A. Guinier and G. Fournet, *Small Angle Scattering of X-Rays* (Wiley, New York, 1955).

[20] B. E. Warren, *X-Ray Diffraction* (Addison-Wesley, London, 1968).

[21] G. Kostorz, in *Treatise on Materials Science and Technology*, edited by G. Kostorz (Academic, New York, 1979), Vol. 15, p. 227.

[22] M. Maruyama, M. Bienfait, F. C. Liu, O. E. Vilches, and F. Rieutord, Surf. Sci. **283**, 333 (1993).

[23] M. Bienfait, J. M. Gay, P. Zeppenfeld, O. E. Vilches, I. Mirebeau, and H. J. Lauter, J. Low Temp. Phys. **111**, 555 (1998).

[24] Manufactured by Le Carbone Lorraine, Departement Produits Spéciaux, 37 à 41 rue Jean Jaurès, F-92231 Gennevilliers, France.

[25] A. Thomy and X. Duval, J. Chim. Phys. Phys.-Chim. Biol. **67**, 1101 (1970).

[26] M. H. W. Chan, A. D. Migone, K. D. Miner, and Z. R. Li, Phys. Rev. B **30**, 2681 (1984).

[27] A. Guinier, *X-Ray Diffraction* (Freeman, San Francisco, 1963).

[28] P. W. Stephens, P. A. Heiney, R. J. Birgeneau, P. M. Horn, D. E. Moncton, and G. S. Brown, Phys. Rev. B **29**, 3512 (1984). We have used this method for analyzing our data. A similar formalism, specifically for neutron-scattering experiments, was developed earlier by J. K. Kjems, L. Parsell, H. Taub, J. G. Dash, and A. D. Novaco, Phys. Rev. B **13**, 1446 (1976).

[29] M. Bienfait and J. M. Gay, in *Phase Transition in Surface Films 2*, edited by H. Taub *et al.* (Plenum Press, New York, 1991), p. 307.

[30] H. P. Schildberg, H. J. Lauter, H. Freimuth, H. Wiechert, and R. Haensel, Jpn. J. Appl. Phys., Part 1 **26**, 345 (1987); H. J. Lauter, V. L. P. Frank, H. Taub, and P. Leiderer, Physica B **165-166**, 611 (1990); H. J. Lauter, H. Godfrin, V. L. P. Frank, and P. Leiderer, in *Phase Transitions in Surface Films 2*, edited by H. Taub *et al.* (Plenum Press, New York, 1991), p. 135.

[31] E. V. L. de Mello and M. S. O. Massunaga, Surf. Sci. **199**, 579 (1988).